



ChemComm

**Efficient and Selective Carbon-Carbon Coupling on Coke-Resistant PdAu Single-Atom Alloys**

Journal:	<i>ChemComm</i>
Manuscript ID	CC-COM-10-2019-007932.R1
Article Type:	Communication

SCHOLARONE™  
Manuscripts

## COMMUNICATION

## Efficient and Selective Carbon-Carbon Coupling on Coke-Resistant PdAu Single-Atom Alloys†

Received 00th January 20xx,  
Accepted 00th January 20xx

Romain Réocreux,<sup>‡a</sup> Matthew Uhlman,<sup>‡b</sup> Theodore Thuening,<sup>b</sup> Paul Kress,<sup>b</sup> Ryan Hannagan,<sup>b</sup> Michail Stamatakis<sup>a</sup> and Charles Sykes<sup>b</sup>

DOI: 10.1039/x0xx00000x

**We demonstrate that PdAu single-atom alloy model catalysts offer a heterogeneous route to selective Würtz-type C-C coupling. Specifically, when methyl iodide is exposed to an otherwise unreactive Au(111) surface, single Pd atoms in the surface layer promote C-I dissociation and C-C coupling, leading to the selective formation of ethane.**

Carbon-carbon (C-C) coupling is a ubiquitous step in chemical transformations. It is often performed using homogeneous palladium catalysts with reaction selectivity tuned by the ligands around the Pd atom. A major drawback with homogeneous Pd catalysts is the recovery of both the catalyst and the often expensive ligands upon separation of the products.<sup>1,2</sup> These Pd complexes can also be toxic and require harsh conditions to facilitate Ullmann-type C-C coupling.<sup>3</sup> Since these C-C coupling reactions are most often catalysed by sometimes-problematic homogeneous methods, there is a great interest in discovering heterogeneous routes that offer much greater ease of separation of products and catalyst recovery. There have been previous reports that Pd nanoparticles are active for C-C coupling, but the active site for the coupling is still debated.<sup>4</sup> The role of the metal surface in catalysing coupling reactions has been examined using the tools of surface science and these experiments have investigated several different coupling reactions including Ullmann,<sup>5,6</sup> Würtz,<sup>7</sup> Sonogashira,<sup>8</sup> and Suzuki-Miyaura.<sup>9</sup> This approach to these complex reactions is particularly powerful as it enables identification of active sites on the surface and can yield a direct correlation of site type with reaction pathway. Of particular interest is the coupling of two sp<sup>3</sup> carbons, which has remained a relatively challenging synthetic route.<sup>10</sup>

Recently there have been advances in using Pd active sites in heterogeneous catalysts at their smallest ensemble size by isolating single Pd atoms and anchoring them on a various supports.<sup>11,12</sup> This method has been demonstrated to be more active for Sonogashira coupling and Suzuki-Miyaura couplings relative to the typically used homogeneous catalysts. In an effort to understand how single reactive dopant atoms in the surface of an unreactive metal catalyse reactions, we have investigated fundamental structure-reactivity relationships in ethane production from methyl iodide (MeI) on various PdAu alloys. By combining Scanning Tunnelling Microscopy (STM), Temperature Programmed Desorption (TPD), Density Functional Theory (DFT) and kinetic Monte Carlo (kMC) simulations, we are able to elucidate the atomic-scale structure of the surface, relate this to reaction activity and selectivity, and understand the relevant reaction energetics. We find that pristine Au(111) surfaces are largely inactive towards cleavage of C-I bonds. Introduction of small amounts of Pd in the form of individual, isolated atoms, promotes both the C-I dissociation and sp<sup>3</sup>-sp<sup>3</sup> C-C coupling steps. This C-I bond cleavage has been proposed to be the rate-limiting step on Au(111) for Sonogashira coupling in previous Ultra-High Vacuum studies.<sup>8</sup> At higher coverages of Pd, the coupling channel is suppressed and decomposition pathways dominate. We report via isotope labelling studies and DFT-parameterised kMC simulations that PdAu single-atom alloys (SAA) enable C-I cleavage and subsequent sp<sup>3</sup>-sp<sup>3</sup> coupling of methyl groups without the activation of C-H bonds, which would lead to decomposition (coking) as seen on platinum group surfaces or formation of sp<sup>2</sup> coupling products as seen on Cu surfaces.

In order to examine the reactivity of PdAu(111) alloys towards C-C coupling, we expose a variety of PdAu(111) alloys to deuterated methyl iodide and monitor ethane formation as the crystal is heated. As seen in Figure 1, the Au surface shows negligible activity for this reaction when the deuterated methyl iodide is dosed at 80 K and then heated. Nonetheless, we do see a small amount of ethane formation at 300 K when we expose the Au(111) surface to methyl iodide at 250 K.

<sup>a</sup> Thomas Young Centre and Department of Chemical Engineering, University College London, Roberts Building, Torrington Place, London WC1E 7JE, United Kingdom.

<sup>b</sup> Department of Chemistry, Tufts University, Medford, Massachusetts 02155, United States.

†Electronic Supplementary Information (ESI) available: Computational and Experimental Details, additional data, DFT structures transition states. See DOI: 10.1039/x0xx00000x

‡These authors equally contributed to the work

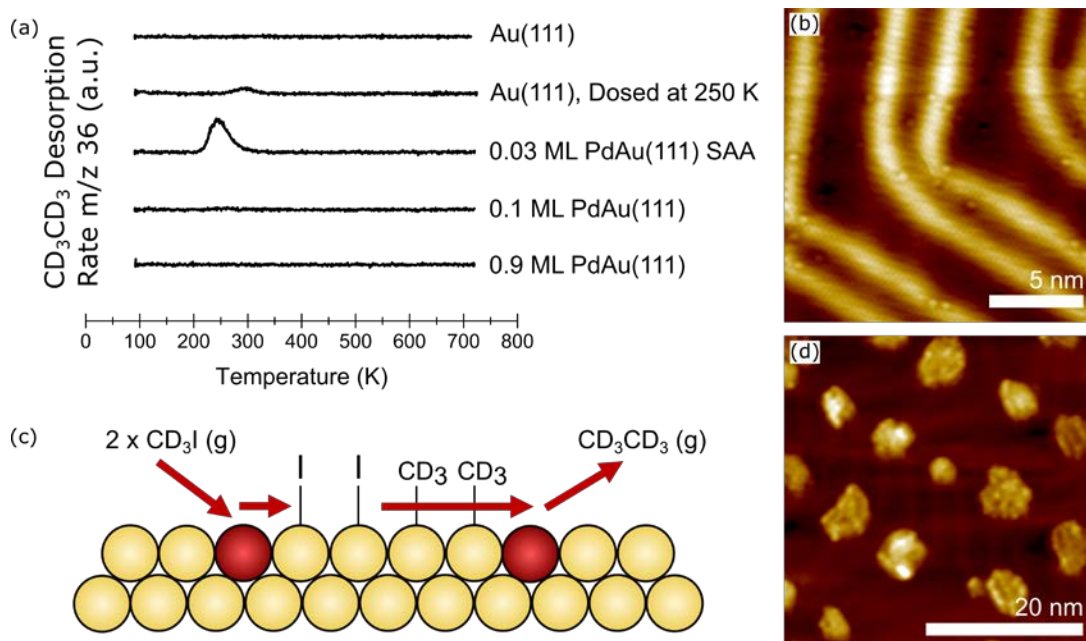


Figure 1: Ethane formation on various PdAu(111) alloys. (a) TPD experiments on Au(111), 3% PdAu(111), 10% PdAu(111), and 90% PdAu(111) surface alloys. Each surface was exposed to 1L  $\text{CD}_3\text{I}$  at 80 K with the exception of the 250 K exposure which was 2 L. (b) STM Image of PdAu(111) SAA. Small white protrusions are the Pd atoms and the larger lines are the so-called herringbones of the  $22\times\sqrt{3}$  reconstruction of Au(111). The points at which the herringbones change direction contain an edge dislocation defect. (c) Schematic of the proposed reaction mechanism. (d) STM Image of PdAu(111) showing extended Pd ensembles in the form of one atom high islands on the Au(111) surface.

Similar activity on Au(111) has been observed in previous work by Paul and Bent and attributed to defects in the Au surface that facilitate C-I cleavage supplying methyl groups which couple to form ethane.<sup>13</sup> Most interestingly, we find that small amounts of Pd (3 % surface composition) promote both the initial C-I cleavage and the coupling of methyl groups. At these coverages, the Pd sites exist in the form of a PdAu(111) SAA.<sup>14</sup> It is known that Pd atoms alloy into the surface at the edge dislocations of the herringbone reconstruction of Au(111), which leads to a higher local concentration of isolated Pd atoms near these herringbone elbow sites as seen in Figure 1b. Exposure of this surface to deuterated methyl iodide results in deuterated ethane desorption at 250 K, *i.e.* 50 K lower than Au(111). At these temperatures, the desorption of ethane is limited by its formation on the surface and the desorption temperature is thus indicative of the activation barrier for ethane formation. Moreover, the fact that we observe more product formation at a lower temperature than Au(111)

indicates that PdAu(111) SAAs facilitate both low-temperature C-I cleavage and C-C coupling, as represented schematically in Figure 1c. At higher Pd coverages, Pd-rich islands are formed, as seen in Figure 1d. Complementary TPD experiments on these higher Pd coverage surfaces (Figure 1a) reveal no ethane formation. This can be attributed to the stronger binding of methyl groups on such extended Pd ensembles, which leads to extensive dehydrogenation of the methyl groups and coking instead of coupling, as discussed later.<sup>15</sup>

Figure 2 displays more detailed TPD traces highlighting how reaction selectivity changes on these different surfaces. On Au(111) dosed at 250 K, we see only a small amount of ethane formation, as previously discussed. On the PdAu(111) SAA, in addition to coupling of  $\text{CD}_3$  to form  $\text{CD}_3\text{CD}_3$ , we also see the production of methane at 200 K with a  $\sim 3:1$  ethane to methane ratio.

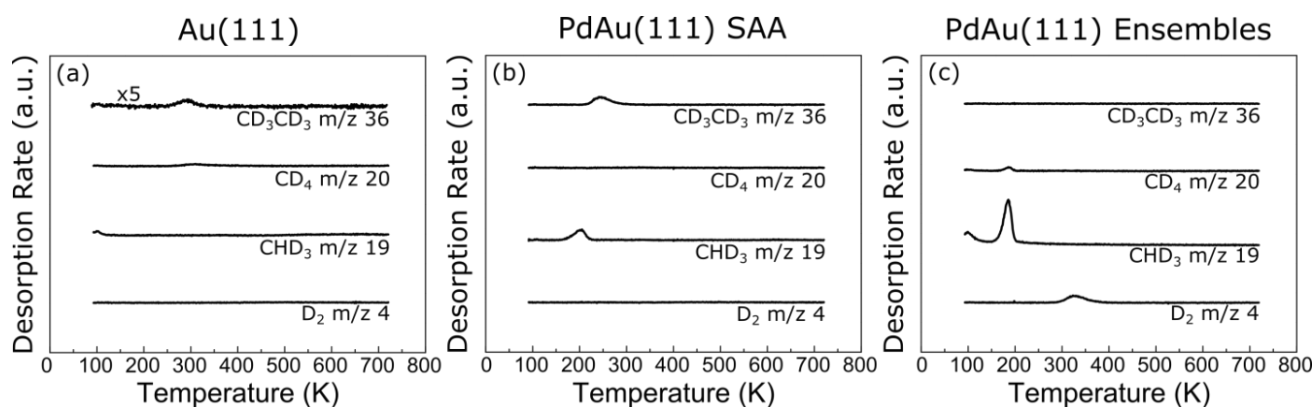


Figure 2: TPD experiments showing selectivity on (a) Au(111), (b) 3% PdAu(111), and (c) 90% PdAu(111) alloys. Each surface was exposed to 1L of  $\text{CD}_3\text{I}$  at 80K.

Table 1: DFT energetics of C-H and C-I cleavages compared to methyl iodine desorption from different Au and PdAu SAA model surfaces. Reaction and activation energies are given in bold and italics respectively (units are eV). ‡ The structures of the transition states are given in Table S1, ESI†.

Elementary step	Au(111)	Au(211)	PdAu(111) SAA	PdAu(211) SAA
MeI → MeI(g)	<b>0.74</b>	<b>0.72</b>	<b>1.08</b>	<b>1.04</b>
MeI → Me+I	0.99 <b>-0.35</b>	0.35 <b>-0.33</b>	0.97 <b>-0.14</b>	0.44 <b>-0.32</b>
CH <sub>3</sub> → CH <sub>2</sub> +H	1.79 <b>1.50</b>	1.36 <b>1.07</b>	1.27 <b>1.14</b>	0.94 <b>0.71</b>

Detection of CHD<sub>3</sub> instead of CD<sub>4</sub> demonstrates that the hydrogenation reaction arises from adsorption of background H<sub>2</sub> and not the activation of a C-D bond in the adsorbed CD<sub>3</sub> groups. As we are able to quantify product desorption to ~0.3% ML we are confident that negligible C-D activation leading to methane occurred. This is consistent with previous work which showed that PdAu(111) SAAs are indeed capable of H<sub>2</sub> activation.<sup>16–18</sup> At higher coverages of Pd, when ensembles containing Pd-Pd bonds are present,<sup>19</sup> we also observe hydrogenation of the CD<sub>3</sub> groups via background H<sub>2</sub>; however, in contrast to the SAA system, on extended Pd ensembles we observe decomposition of the CD<sub>3</sub> groups via C-D activation leading to CD<sub>4</sub> and D<sub>2</sub> formation. Unlike Au and PdAu SAAs, no ethane was observed from the high coverage PdAu(111) surfaces, indicating that the C-C coupling channel is unique to Pd in the SAA regime. Because the large Pd clusters bind adsorbates significantly more strongly than a single, isolated Pd atom, the energy required for C-H activation is lower, resulting in the disproportionation of methyl to methane and coke.<sup>15</sup> This is in agreement with early studies on the stability of methyl groups on pure Pd surfaces.<sup>20–22</sup>

Since the selective coupling to ethane is conditional upon the surface dissociation of methyl iodine into iodine and C-H cleavage resistant methyl, we have performed DFT calculations to investigate the reactivity of four model surfaces – namely Au(111), Au(211), PdAu(111) and PdAu(211) – towards C-I cleavage from MeI and C-H cleavage from methyl (see Table 1). On Au(111) the activation energy for the C-I cleavage is ~1 eV, *i.e.* 0.25 eV higher than the desorption energy of methyl iodine,

which would therefore rather desorb than react. This is consistent with our TPD results. Step edges however (modelled by Au(211)) can catalyse the C-I cleavage by lowering the barrier down to 0.35 eV. Similar behaviour is found on PdAu(111) and PdAu(211). But if defects enable the generation of methyl groups, are the latter sufficiently stable to couple towards ethane without reacting further? Our DFT calculations estimate the activation energy of C-H cleavage at ≥1 eV. A similar activation energy was reported on PtCu(111) with C-H activation occurring in methyl groups around 350 K.<sup>23</sup> Therefore, if the coupling occurs at a temperature <350 K, the methyl groups should remain intact.

To get more insight into the C-C coupling step, we performed TPD simulations using a DFT/kMC combined approach (see Figure 3).<sup>24–26</sup> On pure Au(111) the activation energy for the coupling is large, ~1.5 eV (Figure 3a). Step-edges again help with the coupling barrier, which is lowered to ~1 eV (see Figure S1, ESI†) but is still higher than the C-H activation barrier. When alloying the surface with Pd at the single atom limit, methyl groups preferentially coordinate with the Pd dopant atom (stabilisation by 0.16 eV/methyl). This leads us to consider two situations characterised by the methyl to Pd ratio  $\sigma$ . For  $\sigma < 1$ , all methyls are most preferably found atop the dopant. For the coupling to happen, one of the two methyls needs to diffuse to the gold sites (curved arrow in Figure 3a) to approach and react with another methyl atop Pd. The overall activation energy reaches 1.28 eV in this situation. For  $\sigma > 1$ , methyls are available on gold and can diffuse athermally towards another methyl atop Pd. The activation energy is lowered to 1.12 eV (as exempted from the diffusion penalty of

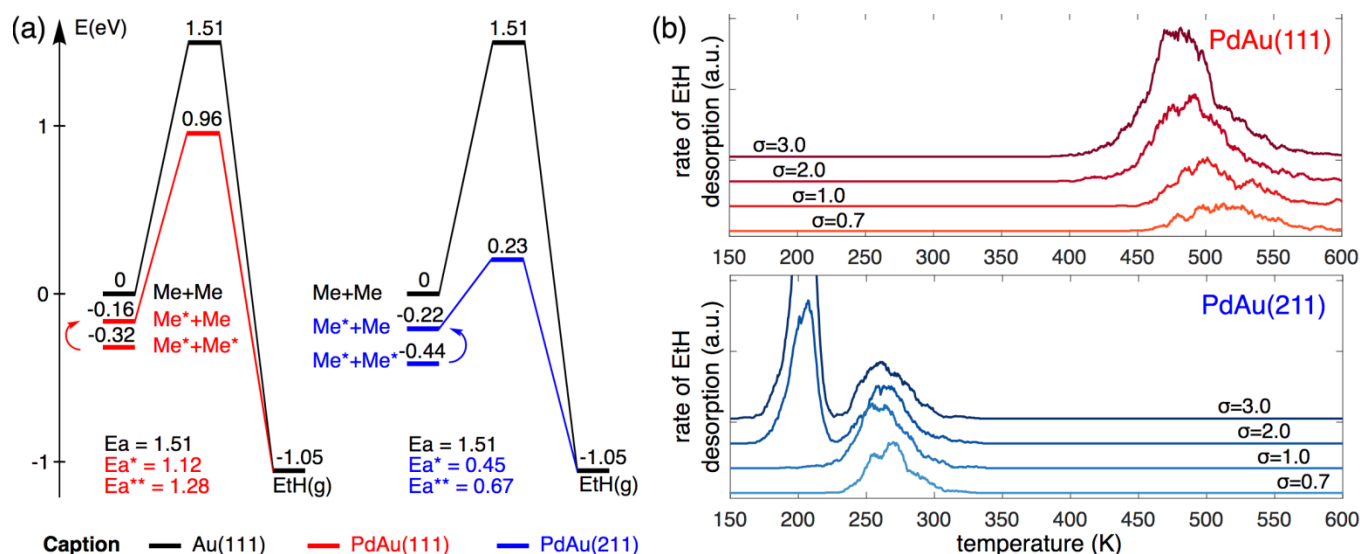


Figure 3: Reactivity of methyl on PdAu single-atom alloys. (a) Energetics of methyl coupling towards ethane computed at the DFT level. Me and Me\* denote methyl adsorbed atop a Au site and a Pd site respectively. The energies are referenced with respect to Me+Me and a clean PdAu model surface ((111) in red and (211) in blue). Ea is the activation energy on Au(111) and Ea\* and Ea\*\* are the activation energies on PdAu from Me\*+Me and Me\*\*+Me\* respectively. (b) KMC-simulated TPD spectra (temperature ramp of 10 K/s) parametrised with the DFT energetics summarised in (a). For each model surface, four sets of simulations are initiated at coverages corresponding to different methyl to Pd ratios (denoted as  $\sigma$ ).

0.16 eV). In spite of this improved catalytic behaviour, the simulations do not show ethane desorbing lower than 460 K (see Figure 3b), in contrast with experimental TPD spectra (250 K). One reason for this discrepancy is the fact that Au(111) exhibits the herringbone reconstruction in which the surface layer is compressed 4.5% with respect to the bulk and the surface contains some undercoordinated Au atoms at edge dislocations. To thus model this type of undercoordinated site, we investigated the reactivity of methyl groups on a single Pd atom embedded at the step-edge of the Au(211) surface. Here, the stabilisation of methyl is greater (-0.22 eV/methyl) and the activation energy is almost three times lower than on Au(111), ranging from 0.45 eV ( $\sigma > 1$ ) to 0.67 eV ( $\sigma \leq 1$ ). For  $\sigma \leq 1$ , the simulated TPD spectra show a unique peak at 255 K, in very good agreement with experimental data. For  $\sigma > 1$ , a second peak appears at 205 K and corresponds to the lower activation energy. This desorption peak is not seen experimentally, indicating that each single Pd atom cannot activate more than one methyl iodine under TPD conditions. This conclusion is supported by the experimental TPD data which show there is only 1 methyl group per Pd atom. These DFT/kMC simulations indicate that the reactive Pd sites are not located on pristine close-packed (111) terraces, but rather at more open and less coordinated environments of edge dislocations. This is consistent with the experimental observation that Pd concentrates at the elbows of the herringbone reconstruction (Figure 1b), where undercoordinated edge dislocation sites are present. It is worth briefly comparing the current study with previous work on PtCu SAAs.<sup>23</sup> When methyl iodide is reacted with PtCu SAAs, the predominant products are methane and ethene, but not ethane. This highlights the current PdAu systems unique ability to perform selective C-C coupling but not C-H activation that leads to one product vs. those seen on PtCu.<sup>23</sup>

In summary, PdAu SAA surfaces offers enhanced catalytic activity and 100% selectivity for sp<sup>3</sup>-sp<sup>3</sup> C-C coupling, a class of reactions that remains challenging. Isolated Pd sites provide lower energy pathways for both C-I cleavage and C-C coupling than Au itself and are superior in performance to extended Pd ensembles which decompose methyl groups. Theory and experiment demonstrate the ability of single Pd atoms to C-C couple but not activate C-H bonds which is key to their promising performance.

This work was supported as part of Integrated Mesoscale Architectures for Sustainable Catalysis, an Energy Frontier Research Center funded by the U.S. Department of Energy, Office of Science, Office of Basic Energy Sciences under Award DE-SC0012573.

## Conflicts of interest

There are no conflicts to declare.

## Notes and references

§ It is worth mentioning that the dissociation proceeds on Au(111), Au(211) and PdAu(211) via an *anti*-insertion transition state, as reported earlier for other leaving groups.<sup>27</sup>

1 N. T. S. Phan, M. Van Der Sluys and C. W. Jones, *Adv. Synth. Catal.*, 2006, **348**, 609–679.

- 2 L. Yin and J. Liebscher, *Chem. Rev.*, 2007, **107**, 133–173.
- 3 F. Monnier and M. Taillefer, *Angew. Chemie - Int. Ed.*, 2009, **48**, 6954–6971.
- 4 J. Durand, E. Teuma and M. Gómez, *Eur. J. Inorg. Chem.*, 2008, **2008**, 3577–3586.
- 5 M. Xi and B. E. Bent, *J. Am. Chem. Soc.*, 1993, **115**, 7426–7433.
- 6 Q. Fan, J. M. Gottfried and J. Zhu, *Acc. Chem. Res.*, 2015, **48**, 2484–2494.
- 7 D. H. Fairbrother, X. D. Peng, R. Viswanathan, P. C. Stair, M. Trenary and J. Fan, *Surf. Sci.*, 1993, **285**, L455–L460.
- 8 V. K. Kanuru, G. Kyriakou, S. K. Beaumont, A. C. Papageorgiou, D. J. Watson and R. M. Lambert, *J. Am. Chem. Soc.*, 2010, **132**, 8081–8086.
- 9 T. Borkowski, A. M. Trzeciak, W. Bukowski, A. Bukowska, W. Tylus and L. Kępiński, *Appl. Catal. A Gen.*, 2010, **378**, 83–89.
- 10 C. P. Johnston, R. T. Smith, S. Allmendinger and D. W. C. MacMillan, *Nature*, 2016, **536**, 322–325.
- 11 X. Zhang, Z. Sun, B. Wang, Y. Tang, L. Nguyen, Y. Li and F. F. Tao, *J. Am. Chem. Soc.*, 2018, **140**, 954–962.
- 12 Z. Chen, E. Vorobyeva, S. Mitchell, E. Fako, M. A. Ortuño, N. López, S. M. Collins, P. A. Midgley, S. Richard, G. Vilé and J. Pérez-Ramírez, *Nat. Nanotechnol.*, 2018, **13**, 1–6.
- 13 A. M. Paul and B. E. Bent, *J. Catal.*, 1994, **147**, 264–271.
- 14 A. E. Baber, H. L. Tierney and E. C. H. Sykes, *ACS Nano*, 2010, **4**, 1637–1645.
- 15 D. Stacchiola, Y. Wang and W. T. Tysse, *Surf. Sci.*, 2003, **524**, 173–182.
- 16 F. R. Lucci, M. D. Marcinkowski, T. J. Lawton and E. C. H. Sykes, *J. Phys. Chem. C*, 2015, **119**, 24351–24357.
- 17 F. R. Lucci, M. T. Darby, M. F. G. Mattered, C. J. Ivimey, A. J. Therrien, A. Michaelides, M. Stamatakis and E. C. H. Sykes, *J. Phys. Chem. Lett.*, 2016, **7**, 480–485.
- 18 M. T. Darby, R. Réocreux, E. C. H. Sykes, A. Michaelides and M. Stamatakis, *ACS Catal.*, 2018, **8**, 5038–5050.
- 19 M. Chen, D. Kumar, C. W. Yi and D. W. Goodman, *Science*, 2005, **310**, 291–293.
- 20 J.-F. Paul and P. Sautet, *J. Phys. Chem. B*, 1998, **102**, 1578–1585.
- 21 F. Solymosi and K. Révész, *J. Am. Chem. Soc.*, 1991, **113**, 9145–9147.
- 22 F. Solymosi and K. Révész, *Surf. Sci.*, 1993, **280**, 38–49.
- 23 M. D. Marcinkowski, M. Darby, J. Liu, J. Wimple, F. R. Lucci, S. Lee, A. Michaelides, Flytzani-Stephanopoulos, M. Stamatakis and E. C. H. Sykes, *Nat. Chem.*
- 24 M. Stamatakis and D. G. Vlachos, *ACS Catal.*, 2012, **2**, 2648–2663.
- 25 J. Nielsen, M. D’Avezac, J. Hetherington and M. Stamatakis, *J. Chem. Phys.*, 2013, **139**, 224706.
- 26 M. Stamatakis and D. G. Vlachos, *J. Chem. Phys.*, 2011, **134**, 214115.
- 27 R. Réocreux, C. A. Ould Hamou, C. Michel, J. B. Giorgi and P. Sautet, *ACS Catal.*, 2016, **6**, 8166–8178.